[Review Paper]

Solid Oxide Fuel Cell as a Multi-fuel Applicable Power Generation Device

Ryuji KIKUCHI* and Koichi EGUCHI

Dept. of Energy and Hydrocarbon Chemistry, Graduate School of Engineering, Kyoto University, Nishikyo-ku, Kyoto 615-8510, JAPAN

(Recieved November 5, 2003)

The solid oxide fuel cell (SOFC) has high conversion efficiency, and is quite attractive from the viewpoint of fuel flexibility, especially the possibility of internal reforming of methane and other hydrocarbons for power generation. The high temperature operation of SOFCs allows the reform of hydrocarbon fuels on the fuel electrode internally in a SOFC module. The power generation characteristics of SOFCs with internal steam reforming of methane were investigated. Steam reforming over a Ni-YSZ (yttria-stabilized zirconia) cermet catalyst attained almost the equilibrium conversion and selectivity in a fixed bed reactor at 1000°C. Internal reforming of hydrocarbons was incomplete because of the limited contact time with the thick layer of the Ni cermet electrode. Therefore, the fuel cell supplied with pre-reformed gas to the anode always produced a lower terminal voltage due to insufficient conversion of the fuel compared with that supplied with post-reformed gas at a given current density. Methane internal reforming proceeded without deterioration with time, whereas power generation with ethane and ethylene was deteriorated by carbon deposition even at high steam-to-carbon ratio. The carbon deposition region and equilibrium partial pressure of oxygen in the C–H–O diagram were estimated from thermodynamic data. The characteristics of CH_4 steam reforming, carbon deposition, and power generation with Ni-YSZ cermet anodes modified by MgO, CaO, SrO, CeO_2, and precious metals were examined. CaO addition was effective for suppressing carbon deposition and promoting CH_4 steam reforming, although the anode electrochemical activity was slightly deteriorated. Ru and Pt addition enhanced steam reforming and suppressed carbon deposition without deteriorating the anode electrochemical activity. The impedance related to gas diffusion was significantly reduced by precious metal additions, indicating that the stability of the anode catalyst was considerably improved since no carbon was deposited.

Keywords

Solid oxide fuel cell, Fuel flexibility, Shift reaction, Steam reforming, Carbon deposition

1. Introduction

Solid oxide fuel cells (SOFCs) are operated at high temperatures and so have advantageous features such as multi-fuel applicability and high conversion efficiency in combination with other power generation systems[1)~5)]. The high operating temperature allows the reform of hydrocarbon fuels both internally on the fuel electrode and externally in a reformer. In principle, reforming of the fuel could lead to higher conversion efficiency, because the thermal energy emitted in the electrochemical reaction is chemically recuperated by the endothermic steam reforming reaction. In particular, internal reforming is expected to be more effective for chemical recuperation, since the reforming reaction temperature is as high as the operation temperature of SOFCs and thus degradation of the thermal energy can be minimized. In the internal reforming operation, a mixture of steam and various fuels such as hydrocarbons and alcohols is introduced directly to the fuel electrode for power generation and the fuel species are catalytically converted *via* a steam reforming reaction into a mixture of H_2, CO, H_2O and CO_2 over a Ni-YSZ (yttria-stabilized zirconia) cermet catalyst used as the anode.

Carbon monoxide, which is a poison for fuel cells operated below 200°C, can be utilized effectively as a fuel in SOFCs. During the internal reforming of methane, for example, the fuel electrode is exposed to gaseous mixtures of CH_4, H_2, H_2O, CO, and CO_2. The reactivity of these gas species in the electrochemical and catalytic reactions as well as the diffusion in the electrode pores is crucial in determining the cell performance[4)~7)]. The internal reforming reaction presents problems with the fuel species, active electrocatalysts, reactivity of gas species, efficiency for various fuels, direct reaction of hydrocarbon on the electrode, carbon deposition, and thermal management.

* To whom correspondence should be addressed.
* E-mail: rkikuchi@mbox.kudpc.kyoto-u.ac.jp

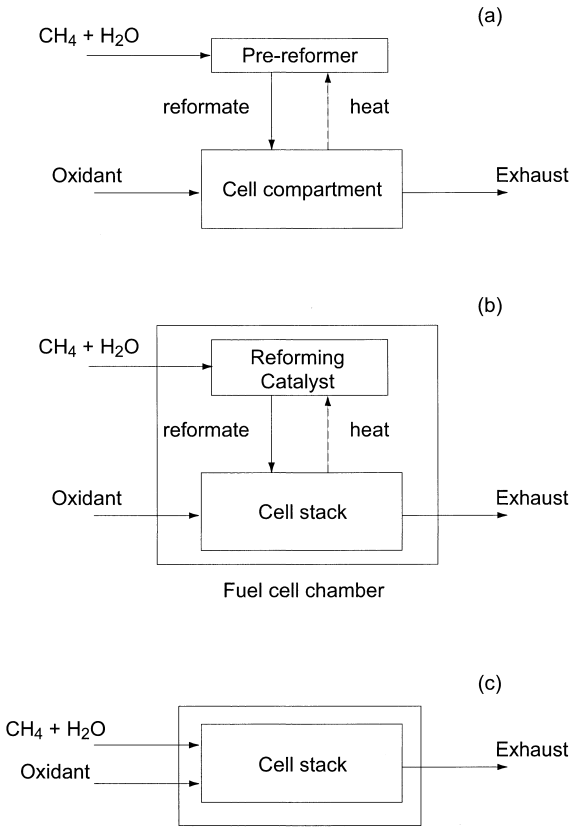

(a) external reforming, (b) indirect internal reforming, (c) direct internal reforming operation.

Fig. 1 Basic Design of Three Types of Hydrocarbon-fueled SOFCs (reproduced from Eguchi (2003)[23])

This study summarizes the basic power generation characteristics of SOFCs during the internal reforming operation with various kinds of fuels, and discusses the electrochemical activity, steam reforming reaction, and shift reaction on conventional and modified Ni-YSZ anodes.

2. External, Direct Internal, and Indirect Internal Reforming

Hydrocarbon fuels are the most suitable fuels for achieving high efficiency in power generation with SOFC from natural resources. Three types of fuel conversions for hydrocarbon fuels can be considered for combination with the reforming reaction as shown in **Fig. 1**[23]. In the external reforming operation (**Fig. 1(a)**), hydrogen is converted in the reformer prior to introduction into the fuel cell chamber. This is the only operation mode for hydrocarbon-fueled polymer electrolyte fuel cells and phosphoric acid fuel cells. In the indirect internal reforming operation (**Fig. 1(b)**), the catalytic reformer is located inside the fuel cell stack, whereas the reforming reaction is carried out in the vicinity of the cell stack but not on the electrode surface. In the direct internal reforming operation (**Fig. 1(c)**), natural gas or hydrocarbon fuel is directly introduced into the cell chamber where the hydrocarbon is converted into hydrogen and carbon monoxide. With the internal reforming operation, heat released from the fuel cell by power generation can be effectively used for the reforming reaction, as the steam reforming of hydrocarbons is largely endothermic.

The Ni-YSZ anode is active for the reforming reaction, so direct reforming can be carried out on the electrode for hydrocarbon-fueled SOFCs. Combination of these methods is also possible. For example, part of the hydrocarbon fuel can be converted in the pre-reformer, then the decomposition of hydrocarbons is completed in the fuel cell chamber or on the fuel electrode. This selection of operational modes depends on heat management, thermal stress, carbon deposition and electrode polarization, cost and system efficiency. In addition to internal reforming, partial oxidation of the hydrocarbon fuel is also possible in the first step of the fuel processing. However, direct introduction of dry fuel for partial oxidation is often associated with carbon deposition. Autothermal reforming, a combination of exothermic partial oxidation and endothermic reforming is another possibility in which the endothermic or thermoneutral condition can be achieved by combination with steam reforming. The above-mentioned reactions for methane can be expressed as

$$CH_4 + x/2O_2 + (1 - x)\,H_2O \longrightarrow CO + (3 - x)\,H_2 \quad (1)$$

where the steam reforming and partial oxidation are $x = 0$ and $x = 1$, respectively. Autothermal reforming is intermediate with $0 < x < 1$.

3. Thermodynamic Considerations

3. 1. Equilibrium Conversion and Selectivity for Steam Reforming, Shift Reaction

The thermodynamic equilibrium of the internal reforming reaction is essential for estimating the conversion and products in internal reforming. The reactions participating in the system are (2), (3), and (4). The steam reforming of methane (2) and water gas shift reaction (3) were taken into consideration:

$$CH_4 + H_2O \longrightarrow CO + 3H_2 \quad (2)$$

$$CO + H_2O \longrightarrow CO_2 + H_2 \quad (3)$$

$$2CO \longrightarrow C + CO_2 \quad (4)$$

The steam reforming reaction (2) is commercially carried out as a catalytic process in chemical plants using supported Ni catalysts at 700-800°C. Since the reforming reaction is a very endothermic reaction, the equilibrium conversion increases as the reaction temperature rises, and reaches almost 100% at 700°C or higher. The selectivity for CO and CO_2 in the reformate depends on the equilibrium of the shift reaction

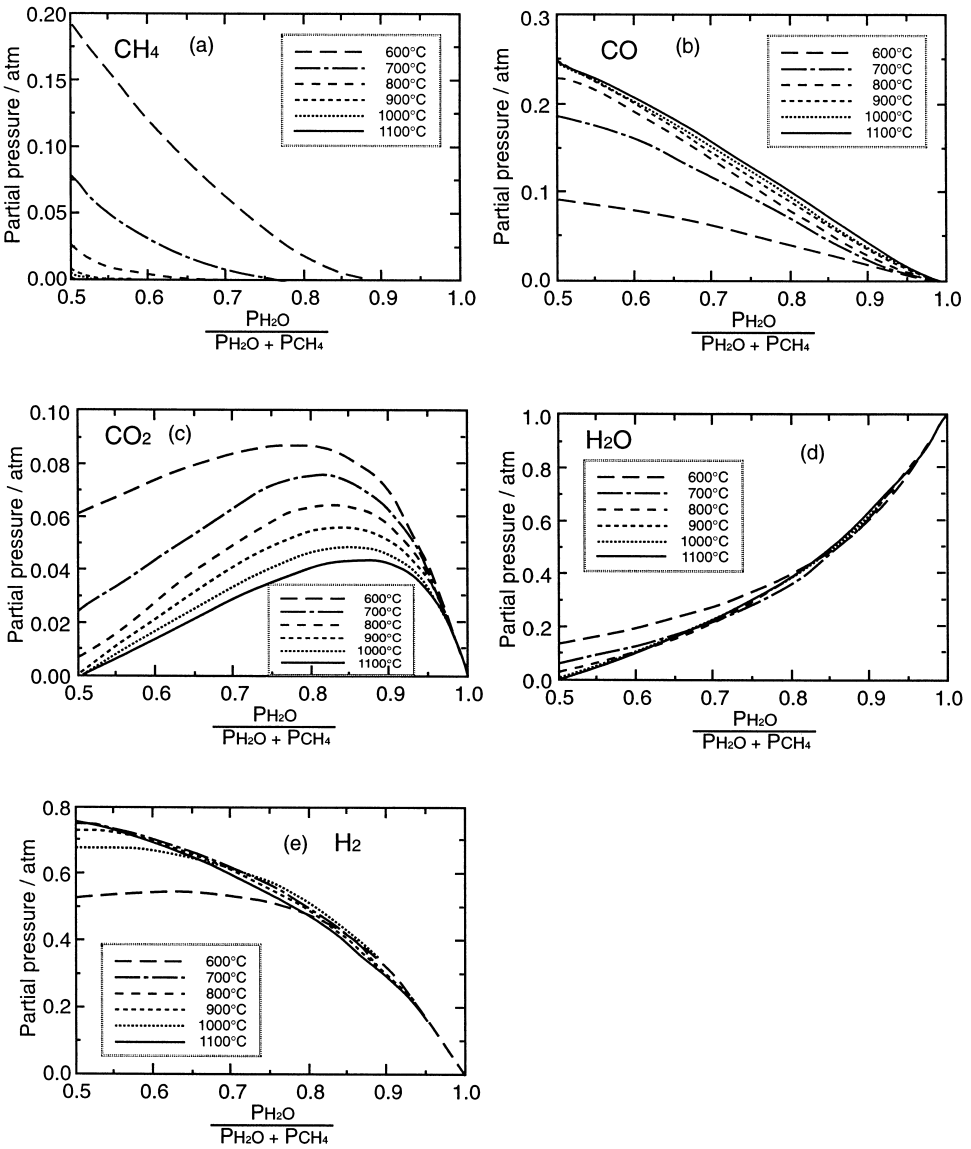

(a) CH_4, (b) CO, (c) CO_2, (d) H_2O, and (e) H_2.

Fig. 2 Equilibrium Composition of Reformed Gas as a Function of Initial $P_{H_2O}/(P_{H_2O} + P_{CH_4})$ (reproduced from Eguchi (2003)[23])

(3). The shift reaction is also used for increasing the hydrogen content from the reformate using Fe–Cr catalyst at around 600°C and Cu–ZnO catalyst at 250°C. Low temperature is favorable for a high hydrogen content because of the exothermic nature of the shift reaction. The carbon formation reaction (4), called the Boudouard reaction, should be avoided, since the deposition of carbon results in pore closure and inefficient supply of the gaseous reactants to the catalytic reaction sites. Therefore, an adequate amount of steam should be added to the hydrocarbon fuel to prevent carbon deposition.

The partial pressures of the five gas components, H_2, H_2O, CO, CO_2, and CH_4, in the thermodynamic equilibrium are shown in **Fig. 2**[23]. The total pressure of the gaseous mixture is 1 atm. The equilibrium conversion of methane increases with the temperature, due to the endothermic nature of the reaction. The conversion reaches *ca.* 100% at 900°C, so the partial pressure of CH_4 should be extremely low at the operation temperature of SOFCs. CO formation is favored with higher temperature because of the exothermic nature of the shift reaction, leading to increased CO selectivity at high temperatures.

3. 2. Carbon Deposition and Partial Pressure of Oxygen in the C–H–O System

Carbon deposition can cause serious reduction of the power generation characteristics of SOFCs as a result

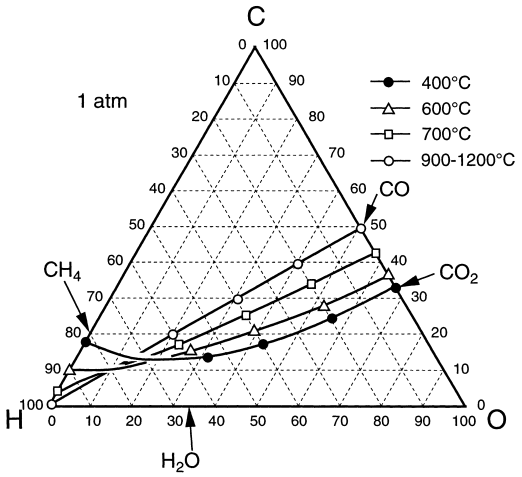

Carbon deposition is expected in the carbon-rich region beyond the boundary at the respective temperatures.

Fig. 3 Boundary of the Carbon Deposition Region in the C–H–O Phase Diagram at 1 atm (reproduced from Takeguchi *et al.* (2002)[8])

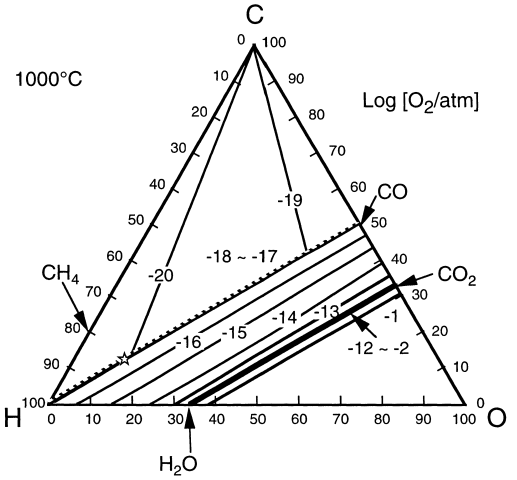

Fig. 4 Equilibrium Partial Pressure of Oxygen in Gas Mixtures in the C–H–O Diagram at 1000°C (reproduced from Takeguchi *et al.* (2002)[8])

of pore closure and encapsulation of the active catalytic sites. As the first step for anticipating carbon deposition, the equilibrium composition of a mixture of H_2O, C (graphite), CO, CO_2, CH_4, H_2, and O_2 was calculated for various molar ratios of C/H/O. The region of carbon deposition in the C/H/O diagram was determined from thermodynamic calculations in the temperature range of 400-1200°C at 1 atm (**Fig. 3**)[8]. At 1000°C or higher, carbon deposition occurs in the C-rich region from the H_2/CO line. The deposition region expands with a decrease in temperature as far as the equilibrium is concerned. CH_4 becomes stable at low temperatures resulting in bending of the boundary line around the H corner. Therefore, internal operation of the fuel cell in the carbon deposition region should be avoided by adding steam or CO_2, but the kinetic effect should also be taken into account. Carbon deposition can proceed even in the presence of a large amount of steam in the C_2-fueled SOFC.

The equilibrium oxygen partial pressure in the reformed gas mixture at 1000°C was calculated[5)~8)]. The partial pressure of oxygen on the fuel electrode is directly related to the open-circuit voltage (OCV) *via* the Nernst equation. The calculated partial pressure of oxygen is shown in a contour map of the C/H/O diagram (**Fig. 4**)[8]. A drastic change in the partial pressure of oxygen was found when the composition goes to the C- or H-rich side across the CO_2/H_2O line of the stoichiometric composition of combustion. The decrease in partial pressure of oxygen was 10 orders of magnitude on this line. The partial pressure of oxygen was low and gradually decreased along the upper-left direction in the region surrounded by CO, CO_2, H_2, and H_2O, in which the four gas species form a reducing atmosphere. The partial pressure of oxygen dropped on proceeding to the carbon-rich region in which deposition occurs across the CO/H_2 line. The carbon-rich region beyond this line corresponds to carbon deposition at 1000°C as indicated in **Fig. 3**.

4. Steam Reforming of Methane and Shift Reaction on Conventional Ni-YSZ Cermet Catalyst

Steam reforming of methane (2) and the shift reaction (3) on a Ni-YSZ cermet were investigated at atmospheric pressure using a conventional flow system. A commercial YSZ tube painted with the Ni-YSZ cermet supplied by TOTO Ltd. was used for the reaction. The area of the active catalytic surface for the Ni-YSZ cermet on the YSZ tube was 25.8 cm^2. Prior to the reaction, the catalyst was reduced in a 50% H_2/N_2 stream from room temperature to 1000°C at a constant heating rate of 200°C·h^{-1}. Then, the reactants were introduced into the reactor. Reaction products were analyzed by an on-line gas microchromatograph (Chrompack, Micro-GC CP2002). Reaction gas mixture of 22.2% H_2O, 11.1% CO, 33.3% H_2 and 33.4% N_2 was fed at the total rate of 374 m*l*·min^{-1} at standard temperature and pressure (STP). This contact time between reaction gas and Ni-YSZ corresponds to 0.25 s at 1000°C. For steam reforming of methane, the reaction gas mixture consisted of 42.9% H_2O, 14.3% CH_4, and 42.8% N_2 fed at the total rate of 291 m*l* (STP)·min^{-1}. This gas corresponds to the conditions of the steam reforming of methane and the normal operating conditions of SOFCs applied in the power generation test of current density of 300 mA·cm^{-2} and fuel utilization of 60%. The contact time between the reaction

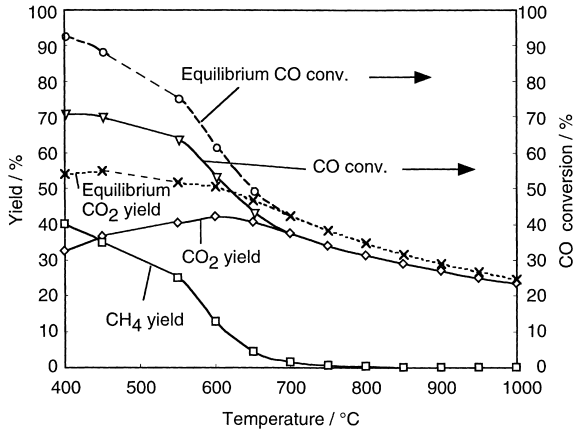

Gas composition: 22.2% H_2O, 11.1% CO, 33.3% H_2, 33.4% N_2; total flow rate of 374 m*l* (STP)·min^{-1}.

Fig. 5 Influence of Reaction Temperature on Shift Reaction (reproduced from Takeguchi *et al.* (2002)[8])

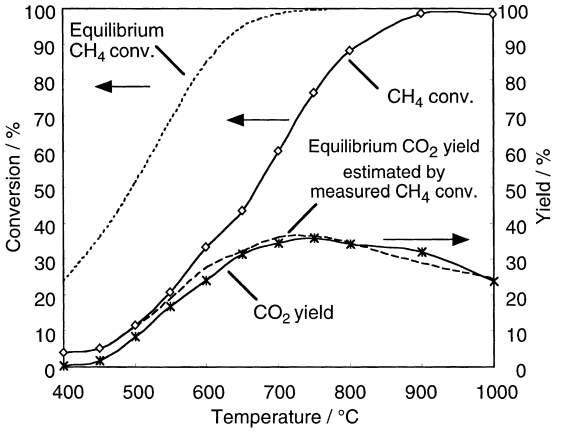

Gas composition: 42.9% H_2O, 14.3% CH_4, 42.8% N_2; total flow rate of 291 m*l* (STP)·min^{-1}.

Fig. 6 Influence of Reaction Temperature on Steam Reforming of Methane (reproduced from Takeguchi *et al.* (2002)[8])

gas and Ni-YSZ corresponds to 0.32 s at 1000°C.

Catalytic activity of the Ni-YSZ cermets for the shift reaction (3) is shown in **Fig. 5**[8]. The equilibrium CO_2 yield and CO conversion in **Fig. 5** were estimated by assuming that four gas species, *i.e.* CO, CO_2, H_2 and H_2O excluding CH_4, were in thermodynamic equilibrium. CO conversion approached the equilibrium at 600°C and reached the equilibrium at over 850°C. The shift reaction is generally accepted to reach equilibrium on transition metal catalysts at relatively low temperatures around 250-300°C. In the present experimental conditions, the shift reaction approached the equilibrium at 550-600°C, but it was difficult to attain the equilibrium conversion due to the very short contact time of 0.25 s. This result indicates that the open circuit voltage below 600°C may deviate from the theoretical value calculated from the partial pressure of O_2 in **Fig. 4** because of the deviation from the equilibrium gas composition.

Steam reforming of methane was investigated as shown in **Fig. 6**[8]. The equilibrium CH_4 conversion reached 100% at 750°C and higher temperatures, while the measured conversion remained far below the equilibrium at temperatures lower than 850°C. Comparison with the results in **Fig. 5** indicates that the rate of CH_4 steam reforming was much slower than that of the shift reaction. The observed conversion was 100% at 900°C, so almost complete conversion could be attained under the operating conditions of SOFCs at 1000°C with a contact time of 0.32 s. This result indicates that the open circuit voltage over 900°C can equal the theoretical value thermodynamically expected from the oxygen partial pressure shown in **Fig. 4**. The measured CO_2 yield agreed well with the calculated value that was obtained by assuming the equilibrium among CO, CO_2, H_2, and H_2O, and excluding CH_4 over the whole temperature range investigated as shown in **Fig. 5**. The shift reaction in **Fig. 6** reached equilibrium more easily than that in **Fig. 5**, indicating that CO formed by the steam reforming was located near the active sites and rapidly reacted with H_2O to form CO_2.

5. Steam Reforming of Ethane and Ethylene on Ni-YSZ Cermet

The behaviors of steam reforming of ethane and ethylene were compared with that of methane. A reaction gas mixture consisting of 46.2% H_2O, 7.7% C_2H_6 (or C_2H_4) and 46.1% N_2 was fed at the total rate of 270 m*l* (STP)·min^{-1}. The contact time between the reaction gas and Ni-YSZ corresponds to 0.34 s at 1000°C. In all cases, the S/C ratio was set at 3. The steam reforming reaction of C_2H_4 and C_2H_6 was carried out as in the case of CH_4. Since both C_2H_4 and C_2H_6 were almost completely converted over 800°C, the CO_2 yield for steam reforming of C_2H_4 and C_2H_6 measured in the range of 800-1000°C is summarized in **Table 1**[8]. The equilibrium CO_2 yield was again calculated, assuming that the four gas species, CO, CO_2, H_2, and H_2O were in thermodynamic equilibrium. The CO_2 yield slightly deviated from the equilibrium even at 800°C for the steam reforming of C_2H_6 and C_2H_4, although that for CH_4 reached equilibrium over 600°C. Steam reforming is generally accepted to initiate *via* the decomposition of hydrocarbons ((5) and (6)), which is the rate-determining step, and will be discussed later:

$$C_2H_4 \longrightarrow 2C + 2H_2 \quad (5)$$

$$C_2H_6 \longrightarrow 2C + 3H_2 \quad (6)$$

Therefore, carbon was deposited on the catalysts after steam reforming even in the carbon free regions shown

Table 1 CO_2 Yield from Steam Reforming of C_2H_4 and C_2H_6 (reproduced from Takeguchi *et al.* (2002)[8])

Fuel	Temperature [°C]	CO_2 yield[a] [C-at.%]	Equilibrium CO_2 yield [C-at.%]
C_2H_4	800	36.8	41.4
	900	33.6	35.3
	1000	29.1	30.6
C_2H_6	800	33.3	37.7
	900	28.2	31.8
	1000	24.4	27.2

Gas composition: 46.2% H_2O, 7.7% C_2H_6 (or C_2H_4), 46.1% N_2; total rate of 270 m*l* (STP)·min^{-1}.
a) Conversion of C_2H_4 and C_2H_6 = 100%.

in **Fig. 2**. The deposited carbon may have covered the active sites, resulting in catalyst deactivation for steam reforming.

6. Power Generation with Internal Reforming of Hydrocarbons and Alcohols

6. 1. Current/voltage Characteristics for Internal and External Reforming of Methane

Current-voltage characteristics of SOFCs with internal reforming of methane were investigated. Cells for power generation experiments were prepared as follows. The Ni-YSZ cermet electrode was prepared by using 80 wt% NiO (Wako Pure Chemical Industries, Ltd.) and 20 wt% YSZ (Tosoh Corp., TZ-8YS). A mixture of these powders was milled for 24 h and calcined at 1400°C in air for 5 h. The resultant cermet powder was mixed with polyethylene glycol to form a slurry. This slurry was applied on one side of a 0.5-mm thick YSZ disk and then the disk was sintered in air at 1400°C. $La_{0.6}Sr_{0.4}MnO_3$ (LSM) and Pt were used as the cathode and reference electrode, respectively, in all experiments unless otherwise noted. LSM powder was prepared using the metal acetates dissolved in water, and then dried at 120°C overnight. The resultant powder was calcined at 900°C for 10 h. The slurry of the powder and polyethylene glycol was painted on a YSZ disk and calcined at 1150°C in air for 5 h.

The internal and external reforming type fuel cell was tested using the experimental apparatus illustrated in **Fig. 7(a)**[24]. A planar cell, prepared as above, was attached to a mullite tube, which was connected to the flow line by a Pyrex glass ring seal (**Fig. 7(b)**). A gaseous mixture of H_2–H_2O, CO–CO_2, or CH_4–H_2O was supplied to the fuel electrode, and pure oxygen to the counter electrode. For external reforming operation, a fixed bed catalytic reactor for steam reforming of methane was connected to the gas entrance of the cell. Two three-way valves switched the gas flow to supply pre- or post-reforming gas to the fuel cell.

Current-voltage characteristics of SOFCs with internal reforming of methane were investigated by supplying pre- and post-reformed gases to the cell (**Fig. 8**[24]). No carbon deposition was expected for this S/C condition as estimated from **Fig. 2**. The catalytic pre-reformer was confirmed to completely convert the CH_4/H_2O mixture to the equilibrium composition. The I/V characteristics of the SOFC supplied with pre- and post-reformed gas are compared in **Fig. 8**. The open circuit voltage (OCV) for the post-reformed gas agreed with that expected for the equilibrium. The open circuit voltage of SOFC supplied with pre-reformed gas was always lower than the corresponding value supplied with the post-reformed gas. The voltage drop with increasing current was also steeper for the case of the pre-reformed gas. This result also implies that the electrode layer is insufficient to convert CH_4 completely, so that the concentrations of H_2 and CO are lower than those in the equilibrium gas after complete reforming. Although equilibrium conversion of CH_4 by steam reforming is generally achieved at 1000°C, insufficient contact time with the Ni/cermet catalyst layer sometimes led to incomplete conversion.

The current/voltage characteristics at different CH_4 concentrations are shown in **Fig. 9(a)**[6]. A high concentration of CH_4 (S/C = 1) resulted in high OCV because of the low oxygen partial pressure of the fuel gas. The shape of the curve changed systematically with CH_4 concentration. The curve with high CH_4 concentration was characterized by a significant concave bending in the small current density region followed by a linear decrease in the terminal voltage with increasing current density. The significant decrease in the low current density region was ascribable to the concentration overvoltage in the vicinity of the ripple-phase boundary. As the small current passed though the electrolyte, H_2O and CO_2 formed *via* power generation significantly enhanced the local oxygen potential. The curves for the low CH_4 concentrations started from a straight decrease and subsequent sharp drop in the terminal voltage in high current density region. This sharp drop is known as the limiting current due to depletion of the fuel in the mixture. Power generation was stable without carbon deposition for the conditions in **Fig. 9(a)**.

The effect of water content in the reaction gas was analyzed at a fixed CH_4 concentration[6]. The current-voltage characteristics at different H_2O concentrations are shown in **Fig. 9(b)**. The OCVs were determined by the steam to carbon ratio. Low H_2O concentration resulted in low oxygen partial pressure in the fuel. The expected values for the oxygen partial pressure agreed with the measured values. The voltage at high current densities was higher for 20% H_2O than for 2% H_2O and 60% H_2O. The low performance of the fuel cell at 2% H_2O can be ascribed to the high polarization resistance and carbon deposition. Internal reforming in this case occurred in the carbon deposition region.

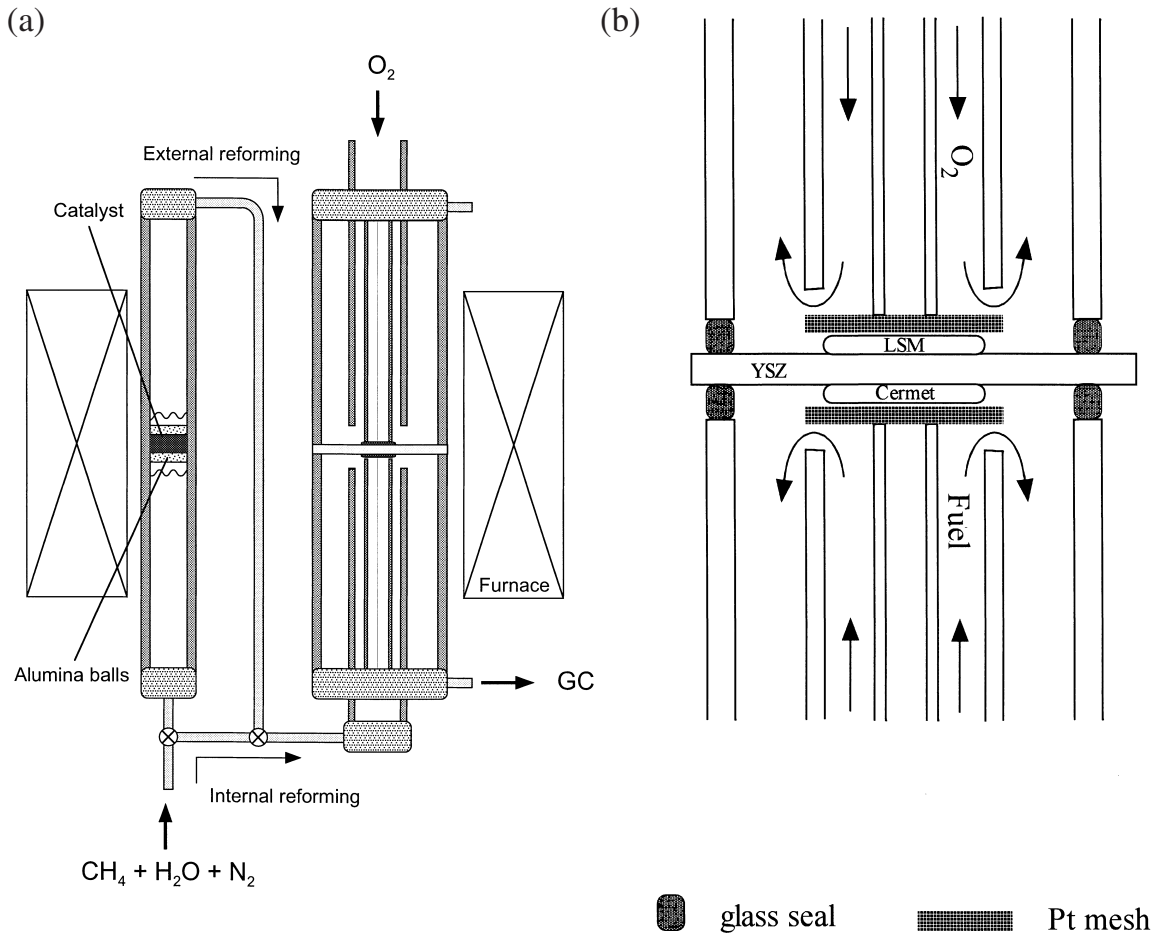

Fig. 7 Schematic Drawing of (a) Fuel Cell Test Bed with a Catalytic Reformer (reproduced from Eguchi *et al.* (2002)[24]), and (b) Detailed Illustration of a Planar Cell Attached to a Mullite Tube with a Glass Seal

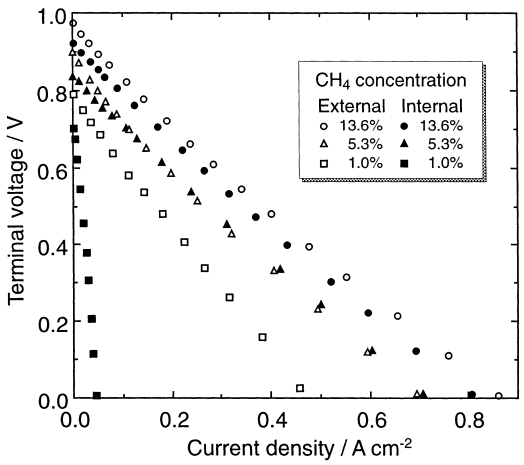

Total gas flow: 100 m*l*·min^{-1}, H_2O: 30.0%, N_2 balance.

Fig. 8 Current-voltage Characteristics for Various CH_4 Concentrations after Internal or External Reforming of CH_4–H_2O Mixtures (reproduced from Eguchi *et al.* (2002)[24])

On the other hand, the low performance at 60% H_2O resulted from the extremely high water content. This result implies that high water concentration during power generation also led to deterioration of the fuel electrode *via* the oxidation of Ni, or adsorption of water or hydroxyl species on the surface. This situation may arise in the downstream region of the cell.

Direct introduction of dry methane to SOFCs has been successful for small-scale cells without carbon deposition[9]. The kinetics of the reaction has been discussed, and direct oxidation of CH_4 at the triple phase boundary has been proposed[10]. The reaction mechanism is complicated since not only the electrochemical reaction of methane but also the secondary CH_4 reforming with steam and CO_2, which is formed by the electrode reaction, may proceed on the Ni surface.

6. 2. Power Generation with Other Hydrocarbons and Alcohols

Power generation with internal reforming of methane did not suffer from deterioration by carbon deposition if the cell was operated in a carbon free region expected from the equilibrium. Carbon deposition became seri-

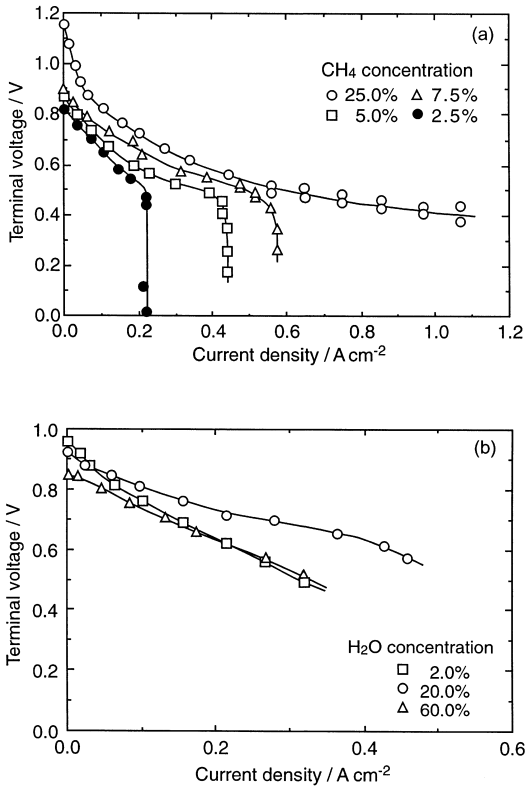

Cell: CH_4/H_2O (30%), Ni-YSZ/YSZ/$La_{0.6}Sr_{0.4}MnO_3$, O_2.
(a) H_2O 25%, (b) CH_4 10%.

Fig. 9 Current-voltage Characteristics of a SOFC with Internal Reforming as a Function of (a) CH_4 and (b) H_2O Concentrations at 1000°C (reproduced from Eguchi *et al.* (1996)[6])

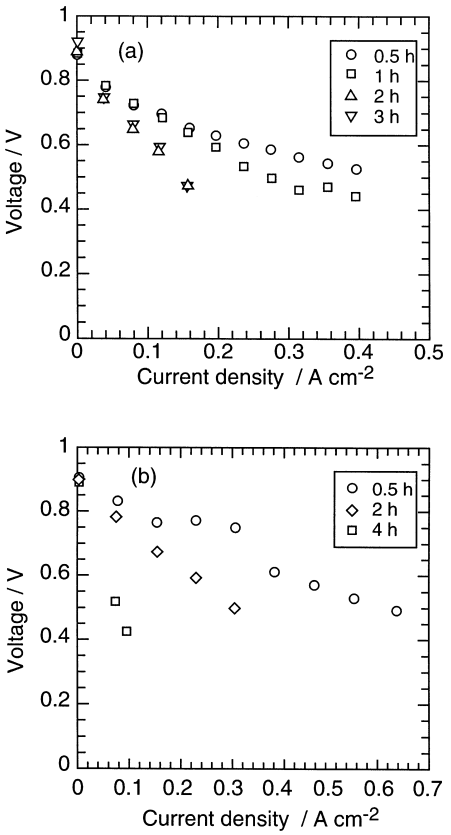

Cell: C_2H_6/H_2O or C_2H_4/H_2O ($H_2O/C = 3.5$), Ni-YSZ/YSZ/$La_{0.6}Sr_{0.4}MnO_3$, O_2.

Fig. 10 Current-voltage Characteristics of (a) Ethane- and (b) Ethylene-fueled SOFCs at 1000°C (reproduced from Eguchi *et al.* (2002)[24])

ous as the carbon number of fuel increased because of carbon residue. The power generation characteristics have been investigated using ethane or ethylene as a fuel as shown in **Fig. 10**[24]. The steam to carbon ratio (S/C = 3.5) was set outside the carbon deposition region. The I-V characteristics were stable for CH_4, *i.e.*, the curve was unchanged with time. On the other hand, the I-V characteristics were deteriorated significantly with time due to carbon deposition using either ethane or ethylene as a fuel. Although a relatively large steam/carbon ratio was employed to avoid carbon deposition, carbon was observed on the Ni electrode and electrolyte after the experiment. Therefore, pre-reforming is necessary for fuels containing C_2 or higher hydrocarbons.

Power generation with methanol fuel can be operated without problem. Only a small amount of water vapor is necessary to avoid carbon deposition. **Figure 11** shows the current/voltage characteristics of a SOFC for various light alcohol-based fuels, as well as for a mixed H_2 and CO fuel[11]. The equilibrium gas compositions were common for the four reaction gas mixtures because the C/H/O atomic ratio of the four gas mix-

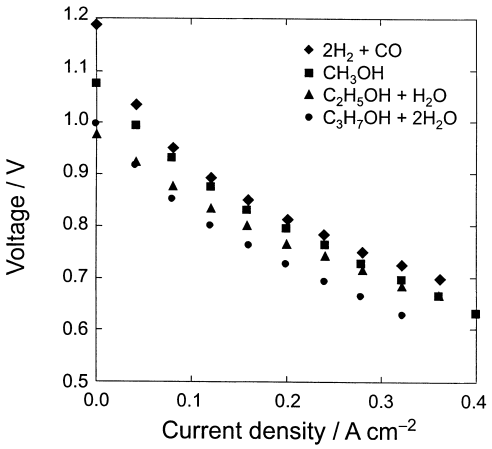

Atomic ratio of C/H/O in the fuel mixtures was fixed at 1 : 4 : 1.

Fig. 11 Current-voltage Characteristics of a SOFC Supplied with Light Alcohol Fuels at 1000°C (reproduced from Sasaki *et al.* (2002)[11])

tures was identical. The OCV was dependent on the type of fuels. The OCV of the mixed H_2 and CO was the highest, and then decreased with increasing carbon number of alcohols from methanol to ethanol and 2-propanol. The reaction rate of direct reforming or decomposition at the electrode catalyst could be different for the alcohols, giving rise to the difference in the OCV. However, except for the 2-propanol-based fuel, the difference in the cell voltage at a given current density for various fuels became smaller with increasing current density, since water formed by the discharge may assist the steam reforming reaction for each fuel. The deterioration of I/V characteristics was obvious for the 2-propanol-fueled SOFC, which was ascribable to carbon deposition.

7. Power Generation Characteristics of SOFCs with Modified Ni-YSZ Cermet Catalysts

The present experimental results demonstrate the potential for internal reforming of hydrocarbon and alcohols in SOFCs. Nevertheless, the activity of anode catalysts for fuel conversion must be further improved. In addition, enhanced fuel electrode performance will be very important for suppressing carbon deposition in power generation with low S/C ratio or higher hydrocarbon and alcohol fuels. Some additives such as alkaline earth oxides and cerium oxide are effective for suppression of carbon deposition in the steam reforming of methane over supported Ni catalysts[12)~14)]. Precious metal catalysts also exhibit excellent activity for steam reforming of methane[15)]. Therefore, addition of these promoters to the Ni-YSZ anode was investigated for suppression of carbon deposition as well as improvement of power generation characteristics.

MgO, CaO, CeO_2, SrO, Ru, Rh, Pd, and Pt were tested as additives to Ni-YSZ. NiO, YSZ, and MgO, CaO, CeO_2 or SrO powders were mixed in the weight ratio of $4 : (1-x) : x$, with $x = 0$, 0.01, 0.05, and 0.10, milled for 24 h, and calcined at 1400°C for 5 h in air. A mixture of NiO and YSZ powders were milled for 24 h, then impregnated with aqueous solution of $Ru(NO_3)_3$, $Rh(NO_3)_3$, $Pd(NO_2)_2(NH_3)_2$, or $Pt(NO_2)_2(NH_3)_2$. The weight ratio of Ni : YSZ : precious metal was fixed at 1 : 0.32 : 0.01. The impregnated powders were calcined at 1400°C for 5 h in air. Cells for power generation using these modified Ni-cermet powders were identical to those for the previous experiments.

In addition to the electrochemical properties of the modified Ni-YSZ cermets, the catalytic activity of the modified cermets for methane decomposition as well as steam reforming of methane was investigated. For methane decomposition, the mixture of the cermet powder and polyethylene glycol was painted on a YSZ disk (8 mm diameter, 0.2 mm thick) as the support. This disk was calcined at 1400°C for 5 h in air, and the thickness of the resultant cermet film was 50 μm (**Fig. 12(a)**). For CH_4 steam reforming, the cermet powders were applied to a YSZ tube as described in Section **4**. The area of the resulting cermet film was 16.3 cm^2 (**Fig. 12(b)**).

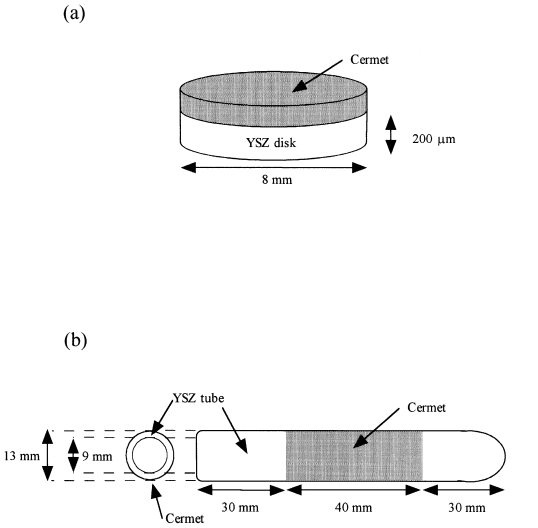

Fig. 12 Schematic Drawing of Catalyst on (a) YSZ Disk and (b) YSZ Tube Used for Carbon Deposition Measurement and for Steam Reforming Reaction of Methane, Respectively

7. 1. Methane Decomposition over the Modified Ni-YSZ Cermet

Methane was decomposed at atmospheric pressure using a thermogravimetric analyzer (Shimadzu Corp., TGA-50), with the catalyst powder loaded in the basket of the balance. Prior to the reaction, catalysts were reduced in the stream of 5% H_2/Ar from the room temperature to 1000°C at a constant heating rate of 10°C·min^{-1}, and the temperature was held at 1000°C for 10 min. Then, the H_2/Ar flow was changed to the flow of 67% methane and 33% N_2. The carbon deposition rate for the first 1 min was given by:

$$= \frac{\text{weight increase by deposited carbon}}{\text{cermet weight} \times \text{reaction period}} \qquad (7)$$

The carbon deposition rates over the Ni-YSZ cermets modified with the alkaline earths are summarized in **Table 2**[8)]. The addition of CaO or SrO to the Ni-YSZ cermet obviously suppressed the carbon deposition, whereas MgO addition to the Ni-YSZ cermet promoted carbon deposition. For CeO_2-modified Ni-YSZ cermet, the rate of carbon deposition was related to the amount of the added CeO, and this will be discussed later. Although NiO in Ni-YSZ cermet is reduced to metallic Ni in the working state of the SOFC, the addition of CaO or SrO with strong basicity modified the

Table 2 Comparison of Decomposition and Steam Reforming of CH_4 Conversion on Various Cermets Modified by Alkaline Earths and CeO_2 (reproduced from Takeguchi *et al.* (2002)[8])

Cermet (before reduction)	Weight ratio	Carbon deposition rate[a] [C-g·cermet-g^{-1}·min^{-1}]	CH_4 conversion[b] [%]		
			600°C	700°C	800°C
NiO : YSZ	4.00 : 1.00	0.045	54.8	90.7	99.3
NiO : YSZ : MgO	4.00 : 0.99 : 0.01	0.056	33.4	67.8	93.8
	4.00 : 0.95 : 0.05	0.046	65.8	91.6	99.3
	4.00 : 0.90 : 0.10	0.049	63.4	92.9	99.3
NiO : YSZ : CaO	4.00 : 0.99 : 0.01	0.024	62.1	91.9	99.2
	4.00 : 0.95 : 0.05	0.027	61.7	91.9	99.2
	4.00 : 0.90 : 0.10	0.024	65.1	93.7	99.4
NiO : YSZ : SrO	4.00 : 0.99 : 0.01	0.032	64.5	93.2	99.4
	4.00 : 0.95 : 0.05	0.031	64.7	92.9	99.3
	4.00 : 0.90 : 0.10	0.031	0.1	0.3	2.7
NiO : YSZ : CeO_2	4.00 : 0.99 : 0.01	0.028	50.5	87.1	98.6
	4.00 : 0.95 : 0.05	0.042	31.3	62.1	86.4
	4.00 : 0.90 : 0.10	0.059	17.6	42.2	70.6

a) Gas composition: 67% CH_4, 33% N_2; total flow rate: 45 m*l* (STP)·min^{-1}; temperature: 1000°C.
b) Gas composition: 40% N_2, 20% CH_4, 40% H_2O; total flow rate: 71.2 m*l* (STP)·min^{-1}.

Table 3 Comparison of Decomposition and Steam Reforming of CH_4 Conversion on Various Cermets Modified by Precious Metals (reproduced from Takeguchi *et al.* (2003)[16])

Cermet (before reduction)	Weight ratio	Carbon deposition rate[a] [C-g·cermet-g^{-1}·min^{-1}]	CH_4 conversion[b] [%]		
			600°C	700°C	800°C
Ni : YSZ	1.00 : 0.32	0.045	54.8	90.7	99.3
Ni : YSZ : Ru	1.00 : 0.32 : 0.01	0.030	65.1	93.6	99.3
Ni : YSZ : Rh	1.00 : 0.32 : 0.01	0.062	57.3	84.5	98.2
Ni : YSZ : Pd	1.00 : 0.32 : 0.01	0.037	57.1	90.3	98.6
Ni : YSZ : Pt	1.00 : 0.32 : 0.01	0.027	62.1	91.3	99.1

a) Gas composition: 67% CH_4, 33% N_2; total flow rate: 45 m*l* (STP)·min^{-1}; temperature: 1000°C.
b) Gas composition: 40% N_2, 20% CH_4, 40% H_2O; total flow rate: 71.2 m*l* (STP)·min^{-1}.

metallic Ni to a slightly cationic state, so carbon deposition was suppressed.

The effect of the precious metal additives on the rate of carbon deposition is summarized in **Table 3**[16]. Addition of Ru, Pd, and Pt reduced carbon deposition, whereas Rh addition promoted carbon deposition. Precious metal-modified Ni catalyst showed high activity and produced a small amount of carbon due to the spill over effect of the precious metal[17]. This experiment suggested that these precious metals had the function of hydrogen spill over, and hydrogen formed by decomposition was spilled over from Ru, Pd and Pt to the carbon species, thus suppressing C–C bond formation.

7. 2. Steam Reforming of Methane over Modified Ni-YSZ Cermet

A gas mixture consisting of 20% CH_4, 40% H_2O and 40% N_2 was fed at the total rate of 71.2 m*l* (STP)·min^{-1} for the steam reforming reaction of methane. The steam-to-carbon ratio used in this experiment was lower than that used in the previous experiments, in order to emphasize the effect of the additives on the steam reforming activity. Catalytic activity was measured at decreasing reaction temperatures from 1000 to 600°C.

Steam reforming is generally accepted to initiate *via* methane decomposition, which is the rate-determining step, at high steam/carbon ratios. The reaction steps are as follows:

$$CH_4 \longrightarrow C + 2H_2 \quad (8)$$

$$C + H_2O \longrightarrow CO + H_2 \quad (9)$$

$$CO + H_2O \longrightarrow CO_2 + H_2 \quad (3)$$

If the reaction rate is proportional to the partial pressure of CH_4, reaction (8) is the rate-determining step. However, reaction (8) is not proportional to the carbon deposition rate. The carbon species, which is the precursor of coke and formed in the steam reforming experiment, was rapidly removed by reactions (3) and (9), so the morphology of the carbon species does not affect the rate of decomposition.

The effect of alkaline earth addition to the Ni-YSZ cermet on steam reforming of CH_4 is also summarized in **Table 2**. No clear correlation was observed between the carbon deposition rate and CH_4 conversion. Therefore, the steam reforming reaction appears to be hindered by either alkaline earth addition or

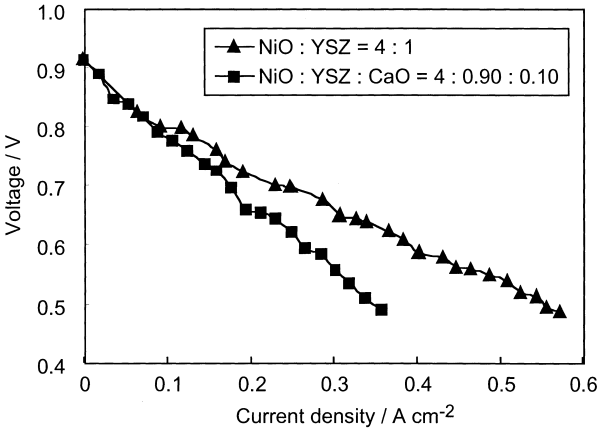

Anode gas: 15% CH_4, 45% H_2O, 40% N_2; flow rate: 150 m*l* (STP)·min^{-1}. Cathode gas: O_2, flow rate: 150 m*l* (STP)·min^{-1}.

Fig. 13 Current-voltage Characteristics in SOFC Operation Using Ni-YSZ and CaO-modified Ni-YSZ Cermets at 1000°C (reproduced from Takeguchi *et al.* (2002)[8])

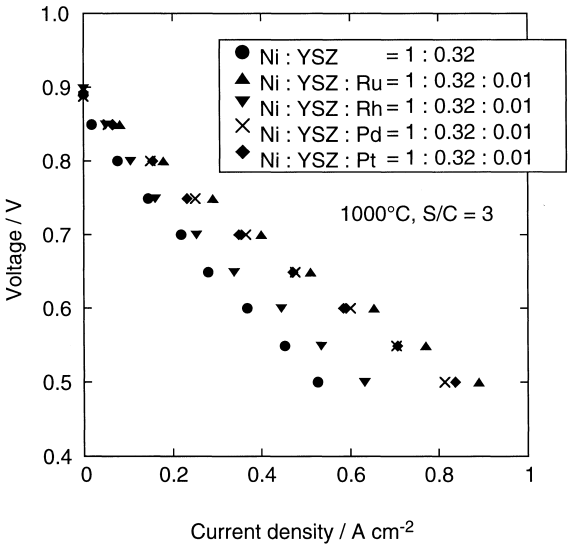

Anode gas: 15% CH_4, 45% H_2O, 40% N_2; flow rate: 150 m*l* (STP)·min^{-1}. Cathode gas: O_2, flow rate: 150 m*l* (STP)·min^{-1}.

Fig. 14 Current-voltage Characteristics in SOFC Operation Using Ni-YSZ and Precious Metal-modified Ni-YSZ Cermets at 1000°C (reproduced from Takeguchi *et al.* (2003)[16])

deposited carbon. Addition of MgO to the Ni-YSZ cermet increased the catalytic activity in the case of $x = 0.05$ or 0.10. Addition of CaO to the Ni-YSZ cermet promoted the activity at every additive level investigated. Addition of SrO to the Ni-YSZ cermet severely deteriorated the catalytic activity at $x = 0.10$. The catalytic activity depended on the amount of CeO_2 added to the Ni-YSZ cermet. Since Ni particles on CeO_2–ZrO_2 solid solutions are stable[18)~21)], Ni-YSZ cermet with low CeO_2 content exhibited a high performance for steam reforming. On the other hand, since CeO_2 components which are not contained in CeO_2–ZrO_2 solid solutions deactivate Ni catalysts[19)], the Ni-YSZ cermet with high CeO_2 content had low activity for steam reforming and produced a large amount of carbon. Among the catalysts modified by the alkaline earths and CeO_2, the CaO-modified Ni-YSZ cermet demonstrated a low carbon deposition rate and high CH_4 conversion for the steam reforming of CH_4.

Addition of any precious metal improved the steam reforming of methane, indicating that the precious metal functioned as the steam reforming catalyst. The precious metals promoted the CH_4 decomposition reaction and H_2 production effectively. Therefore, Ru and Pt addition is effective for promotion of CH_4 reforming as well as for the suppression of carbon deposition.

7. 3. Power Generation Characteristics of Modified Ni-YSZ Cermet

CaO-, Pt-, and Ru-modified Ni-YSZ cermets exhibited lower carbon deposition rates and higher activity for steam reforming of CH_4 than conventional Ni-YSZ cermet, so the effects of these additives on the power generation characteristics with CH_4 were examined. The current-voltage characteristics of SOFCs at 1000°C with S/C = 3.0 using Ni-YSZ and CaO-modified Ni-YSZ cermets are shown in **Fig. 13**[8)]. The ideal open circuit voltage was expected to be 0.95 V based on the data in **Fig. 4**. The open circuit voltage for the cells with Ni-YSZ and CaO-modified Ni-YSZ cermets was 0.92 V, which almost agreed with the expected value. This result indicates that both unmodified and modified cermets functioned as reforming catalysts. Comparing the terminal voltages at a current density of 300 mA·cm^{-2} showed that the voltage of CaO-modified Ni-YSZ cermets was slightly lower than that of Ni-YSZ cermet. Although CaO addition was effective for suppressing carbon deposition and promoting the reforming, the electrochemical activity as the anode was slightly degraded. Alkaline earth oxides are easily dissolved in the cubic zirconia lattice, so the observed deterioration in the power generation characteristics may result from local deviation of the alkaline earth concentration of the electrolyte at the electrocatalytic sites.

Figure 14 shows the current-voltage characteristics of SOFCs at 1000°C with S/C = 3.0 using precious metal-modified Ni-cermet anodes, together with that of the conventional Ni-YSZ cermet anode[16)]. The anode gas composition and flow rate were identical to the condition used in **Fig. 13**, so the thermodynamically expected OCV was 0.95 V. The OCV measured for the cells with the precious metal-modified cermets was about 0.90 V, which was also very close to the theoretical value of 0.95 V. As in the case of CaO-modified Ni-YSZ cermet, the precious metal additives worked

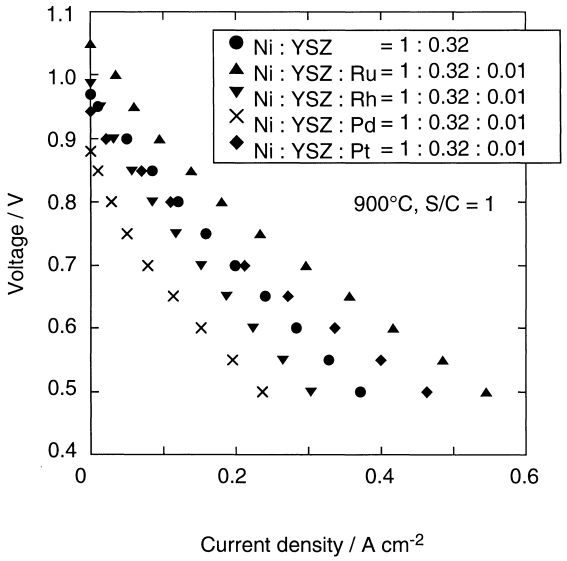

Anode gas: 15% CH_4, 15% H_2O, 70% N_2; flow rate: 150 m*l* (STP)·min^{-1}. Cathode gas: O_2, flow rate: 150 m*l* (STP)·min^{-1}.

Fig. 15 Current-voltage Characteristics in SOFC Operation Using Ni-YSZ and Precious Metal-modified Ni-YSZ Cermets at 900°C (reproduced from Takeguchi *et al.* (2003)[16])

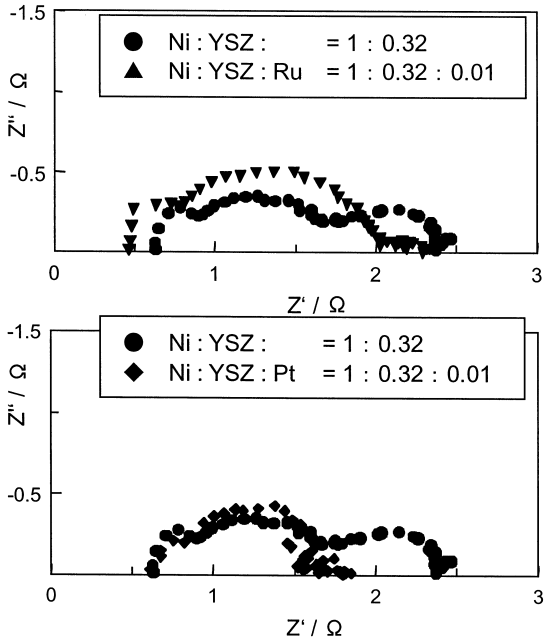

Steam/carbon ratio = 3, bias = open circuit voltage, and applied AC amplitude = 10 mV.

Fig. 16 Impedance Spectra of CH_4-fueled SOFCs at 1000°C Using Ni-YSZ Cermets Modified with Ru and Pt (reproduced from Takeguchi *et al.* (2003)[16])

effectively as reforming catalysts and did not deteriorate the steam reforming activity of the original Ni-YSZ cermet. In the discharging condition, all the precious metal additives promoted electrochemical activity as anode catalysts, although promotion by Rh addition was quite small. With a large steam-to-carbon ratio of 3, the current-voltage curves were almost identical for the cells using the Ru-, Pt-, and Pd-modified Ni-YSZ cermets. However, the Ru additive gave slightly better performance at high current densities than the other two additives.

Figure 15 shows the current-voltage characteristics of the SOFCs at 900°C with a low S/C ratio of 1.0[16]. The improvement in tolerance to carbon deposition by the precious metal additives was more evident in this condition, since this condition was the boundary of carbon deposition as shown in **Fig. 3**. In addition, the effect of carbon deposition on the I/V characteristics could be detected under this condition. OCV varied depending on the cermet under this low S/C condition, whereas the OCV at S/C = 3 and 1000°C was approximately equal to the theoretical value as shown in **Fig. 14**. For this experimental condition, the theoretical value of OCV was estimated to be 1.2 V. The highest OCV was obtained for the cell with the Ru-modified cermet of about 1.05 V, but lower than the theoretical value. This result indicates that steam reforming of methane was incomplete over the modified Ni-YSZ, and consequently the oxygen partial pressure in the vicinity of the triple phase boundary in the fuel electrode was higher than that predicted thermodynamically. However, the Ru-modified cermet improved the OCV compared to the unmodified Ni-YSZ, and the Pt and Ru additives provided much better performance in the discharging condition than the unmodified Ni-YSZ.

7. 4. Impedance Spectra of SOFCs with Pt- and Ru-modified Cermet

Impedance spectra for the CH_4-fueled SOFCs using Ni-YSZ cermets modified with Ru and Pt are shown in **Fig. 16**. The SOFC was operated at the same conditions as shown in **Fig. 14**[16]. The impedance measurements were carried out over the frequency range of 0.01 to 10^6 Hz with 10 mV AC under open circuit conditions using a frequency response analyzer (Solartron 1260). For Ni-YSZ, this plot had one large semicircle with resistance of *ca.* 1.5 Ω and one small semicircle with resistance of *ca.* 0.7 Ω. The characteristic frequencies defined as $\omega = (R \cdot C)^{-1}$ at the summits of the semicircles were *ca.* 1000 and 20 Hz, respectively. Since the high-frequency and low-frequency semicircles were ascribed to the electrochemical reaction and gas diffusion, respectively[22], the large semicircle could be related to the reaction process, and the small semicircle to the gas diffusion process. For Ru and Pt-modified Ni-YSZ, the small semicircle disappeared, but the large semicircle did not change. This result indicates that Ru and Pt addition did not affect the impedance caused by the reaction, but greatly reduced the

impedance caused by the gas diffusion. Steam reforming of methane on the Ni-YSZ modified with Ru and Pt was rapid as shown in **Table 3**, so the carbonaceous species, which is the precursor of coke, was effectively converted by reaction (9). Therefore, the hydrogen supply was rapid due to the deficiency of carbonaceous species or coke. Effective conversion of the carbonaceous species is important to promote electrochemical activity. These results show that the modified anode was quite stable without problems caused by coke formation.

8. Conclusion

The chemical basis of the internal reforming operation of SOFCs and the experimental results for the SOFCs with internal reforming were investigated. Internal reforming of methane can proceed over the electrode layers of Ni-YSZ, but an adequate amount of catalysts is needed to attain full conversion. For multi-component fuels originating from carbonaceous fuels, the reactivity of the catalyst for internal reforming or fuel conversion should also be considered, in addition to the electrochemical oxidation. Carbon deposition is another factor in determining the current-voltage characteristics of the SOFC. In addition to the thermodynamic condition for carbon deposition, the kinetic effect is an important factor, especially for C_2 or larger fuels. Additives to the cermet significantly affected the kinetic parameters of steam reforming of CH_4 as well as carbon deposition on Ni-YSZ cermet. CaO-, Pt-, and Ru-modified Ni-YSZ cermets were effective for suppressing carbon deposition without deteriorating the reforming activity. CaO addition to Ni-YSZ resulted in a slight degradation in power generation characteristics, whereas the precious metal additives such as Pt and Ru promoted the electrochemical activity, and decreased the impedance related to gas diffusion.

Further investigation is needed to clarify the mechanisms of the reforming reaction, carbon deposition, and deactivation, in order to design an active and stable fuel electrode material for internal reforming. The design of the internal reforming SOFC should also be investigated to achieve the maximum practical efficiency from hydrocarbons and other fuels.

Acknowledgment

The present work was partially supported by a Grant-in Aid for scientific research from the Ministry of Education, Culture, Sports, Science and Technology, Japan, by the Dept. of Core Research for Evolutional Science and Technology (CREST) of Japan Science and Technology Corporation (JST), and by International Joint Research Program grant (No.2001EF004) awarded by the New Energy and Industrial Technology Development Organization (NEDO).

References

1) Ringel, H., Schüle, J., Grunwald, D., 'SOFC design with internal heat exchange and gas reforming,' Proc. 5th Int. Symp. Solid Oxide Fuel Cells, eds. by Stimming, U., Singhal, S. C., Tagawa, H., Lehnert, W., PV 97-18, The Electrochem. Soc., Pennington, NJ (1997), p. 124.
2) Divisek, J., Lehnert, W., Meusinger, J., Stimming, U., Proc. 5th Int. Symp. Solid Oxide Fuel Cells, eds. by Stimming, U., Singhal, S. C., Tagawa, H., Lehnert, W., PV 97-18, The Electrochem. Soc., Pennington, NJ (1997), p. 993.
3) Finnerty, C. M., Cunningham, R. H., Ormerod, R. M., Proc. 6th Int. Symp. Solid Oxide Fuel Cells, eds. by Singhal, S. C., Dokiya, M., PV 99-19, The Electrochem. Soc., Pennington, NJ (1999), p. 568.
4) Eguchi, K., Nishiyama, J., Sekizawa, K., Yamada, K., Proc. 6th Int. Symp. Solid Oxide Fuel Cells, eds. by Singhal, S. C. Dokiya, M., PV 99-19, The Electrochem. Soc., Pennington, NJ (1999), p. 1010 .
5) Eguchi, K., Kunisa, Y., Adachi, K., Arai, H., *J. Electrochem. Soc*., **143**, 3699 (1996).
6) Eguchi, K., Kunisa, Y., Kayano, M., Sekizawa, K., Yano, S., Arai, H., *Denki Kagaku*, **64**, 596 (1996).
7) Eguchi, K., Kayano, M., Kunisa, K., Arai, H., "A study on fuel electrode materials for solid oxide fuel cells," Proc. 4th Int. Symp. Solid Oxide Fuel Cells, eds. by Dokiya, M., Yamamoto, O., Tagawa, H., Singhal, S. C., PV 95-1, The Electrochem. Soc., Pennington, NJ (1995), p. 676.
8) Takeguchi, T., Kani, Y., Yano, T., Kikuchi, R., Eguchi, K., Tsujimoto, K., Uchida, Y., Ueno, A., Omoshiki, K., Aizawa, M., *J. Power Sources*, **112**, 588 (2002).
9) Aida, T., Abudula, A., Ihara, M., Komiyama, H., Yamada, K., 'Direct oxidation of methane on anode of solid oxide fuel cell,' Proc. 4th Int. Symp. Solid Oxide Fuel Cells, eds. by Dokiya, M., Yamamoto, O., Tagawa, H., Singhal, S. C., PV 95-6, The Electrochem. Soc., Pennington, NJ (1995), p. 801.
10) Ihara, M., Kawai, T., Matsuda, K., Yokoyama, C., 'Similarity and difference of DC polarization characteristics and electrode reactions between Ni/YSZ anodes and Pt/YSZ anodes in SOFC with dry CH_4 fuel,' Proc. 7th Int. Symp. Solid Oxide Fuel Cells, eds. by Yokokawa, H., Singhal, S. C., PV 2001-16, The Electrochem. Soc., Pennington, NJ (2001), p. 684.
11) Sasaki, K., Kojo, H., Hori, Y., Kikuchi, R., Eguchi, K., *Electrochemistry*, **70**, 18 (2002).
12) Quincoces, C. E., Dicundo, S., Alvarez, A. M., Gonzalez, M. G., *Mater. Lett*., **50**, 21 (2001).
13) Frusteri, F., Arena, F., Calogero, G., Torre, T., Parmaliana, A., *Catal. Commun*., **2**, 49 (2001).
14) Choudhary, V. R., Uphade, B. S., Mamman, A. S., *J. Catal.*, **172**, 281 (1997).
15) Kikuchi, E., Tanaka, S., Yamazaki, Y., Morita, Y., *Bull. Jpn. Petrol. Inst.*, **16**, (2), 95 (1974).
16) Takeguchi, T., Kikuchi, R., Yano, T., Eguchi, K., Murata, K., *Catal. Today,* **84**, 217 (2003).
17) Inui, T., Takeguchi, T., Matsuoka, I., *Current Topics Catal*., **2**, 73 (1999).
18) Nakagawa, N., Sagara, H., Kato, K., *J. Power Sources,* **92**, 88 (2001).
19) Takeguchi, T., Furukawa, S., Inoue, M., *J. Catal*., **202**, 14 (2001).
20) Roh, H.-S., Jun, K.-W., Dong, W.-S., Chang, J.-S., Park, S.-E., Joe, Y.-I., *J. Mol. Catal. A: Chem*., **181**, 137 (2002).
21) Zhuang, Q., Qin, Y., Chang, L., *Appl. Catal*., **70**, 1 (1991).
22) Primdahl, S., Mogensen, M., *J. Electrochem*., **146**, 2827 (1999).

23) Eguchi, K., 'Internal Reforming,' "Handbook of Fuel Cells - Fundamentals, Technology and Applications," eds. by Vielstich, W., Gasteiger, H. A., Lamm, A., Volume 3, John Wiley & Sons, West Sussex (2003), p. 1057.
24) Eguchi, K., Kojo, H., Takeguchi, T., Kikuchi, R., Sasaki, K., *Solid State Ionics*, **152-153**, 411 (2002).

要　　旨

固体酸化物形燃料電池—内部改質発電と燃料適応性—

菊地　隆司，江口　浩一

京都大学大学院工学研究科物質エネルギー化学専攻，615-8510 京都市西京区京都大学桂

固体酸化物形燃料電池（SOFC）は，高温作動のため高い変換効率が期待でき，また多様な燃料を用いて発電できるという燃料適応性がある。メタンやその他の炭化水素燃料では，電極に用いられたNiを触媒とし，直接電極上で燃料を改質する内部改質型の発電が可能である。本研究ではSOFCにおけるメタンの内部改質型発電特性について研究を行った。固定床流通式反応器を用いた反応実験では，Ni-YSZ（Yttria-Stabilized Zirconia）サーメット上でのメタン水蒸気改質反応は，1000℃でほぼ平衡に達した。他の炭化水素の改質反応は，平衡に到達せず，これはNi-YSZサーメットが厚膜状で，接触時間が短いことによる。したがって，燃料ガスを直接発電セルに導入した場合には，改質ガスを供給した場合と比較して，常に端子電圧が低くなった。メタンの内部改質発電では発電特性の劣化は見られなかったが，燃料としてエチレンやエタンを用いた場合には，水蒸気／炭素比が高い条件でも炭素析出が起こり，発電特性の劣化が起こった。Ni-YSZにMgO，CaO，SrO，CeO_2や貴金属を添加し，水蒸気改質反応の活性向上，炭素析出抑制効果，発電特性の向上を検討した。CaOの添加は，水蒸気改質反応活性向上および炭素析出抑制に効果があったが，発電特性は若干低下した。貴金属添加物の中では，Ru，Ptに炭素析出抑制効果があり，また水蒸気改質反応活性および発電特性の向上が見られた。貴金属添加電極を用いたセルのインピーダンス測定により，Ru，Ptの添加でガス拡散に伴う抵抗成分が著しく低下することが明らかとなった。これらのセルでは炭素析出による多孔質電極の閉そくがほとんど起きないと予想され，安定した発電が可能になると考えられる。